

## Supplementary Information

### **Enhanced Thermal Reliability of p-type PbTe Thermoelectric Devices through Interfacial Design with FeCoNiCr Multicomponent Diffusion**

#### **Barrier**

Lianghan Fan,<sup>a,b</sup> Zongwei Zhang,<sup>\*b</sup> Chuandong Zhou,<sup>b</sup> Zhoumin Jiang,<sup>a,b</sup> Ruijie Li,<sup>b,c</sup> Qiang Zhang,<sup>b</sup> Liya Miao,<sup>b,c</sup> Rensheng Zhang,<sup>b</sup> Jianfeng Cai,<sup>b</sup> Guo-Qiang Liu,<sup>b,c</sup> Xiaojian Tan,<sup>\*b,c</sup>  
Jun Jiang<sup>\*b,c</sup>

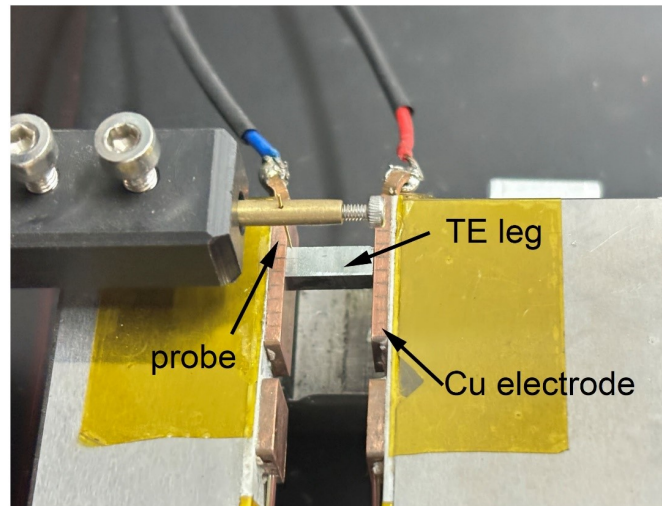
<sup>a</sup> *School of Material Science and Chemical Engineering, Ningbo University, Ningbo 315211, China.*

<sup>b</sup> *Ningbo Institute of Materials Technology and Engineering, Chinese Academy of Sciences; Ningbo 315201, China.*

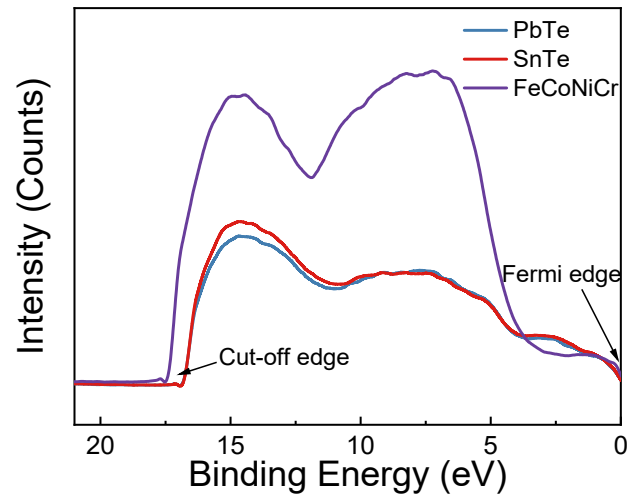
<sup>c</sup> *University of Chinese Academy of Sciences Beijing, 100049, China.*

\*Corresponding authors and Emails: zhangzongwei@nimte.ac.cn; tanxiaojian@nimte.ac.cn;

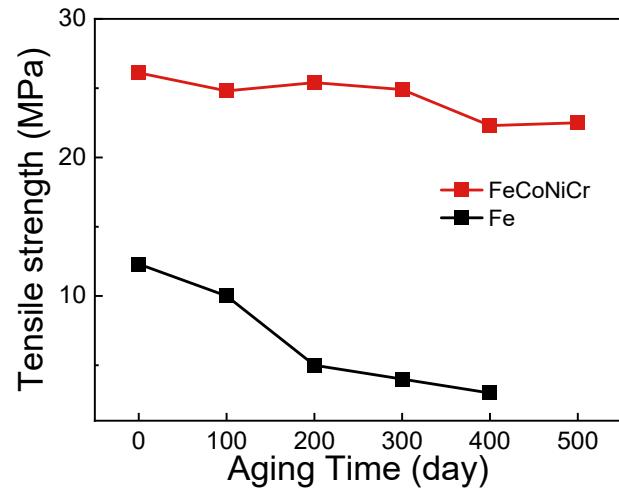
jjun@nimte.ac.cn.



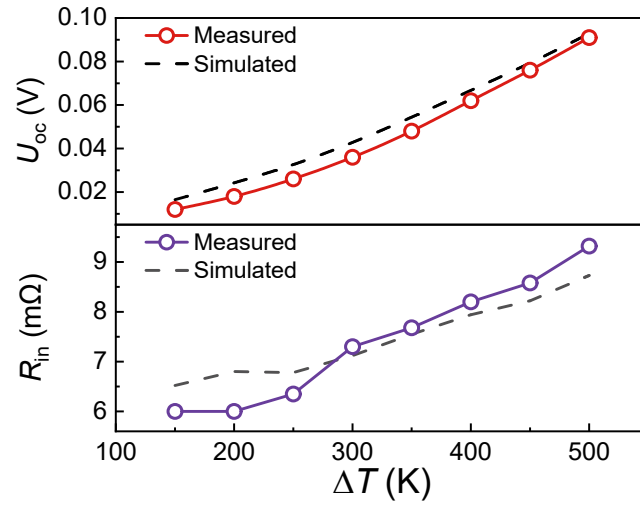
**Supplementary Figure S1.** The schematic diagram of the four-probe measurement device.



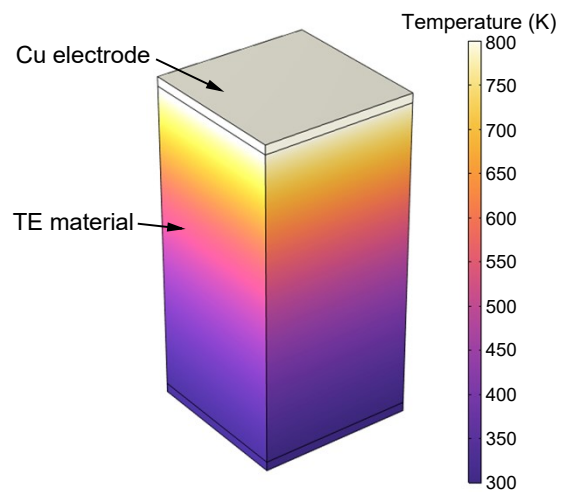
**Supplementary Figure S2.** The UPS spectrum for the p-type PbTe, SnTe, and FeCoNiCr.



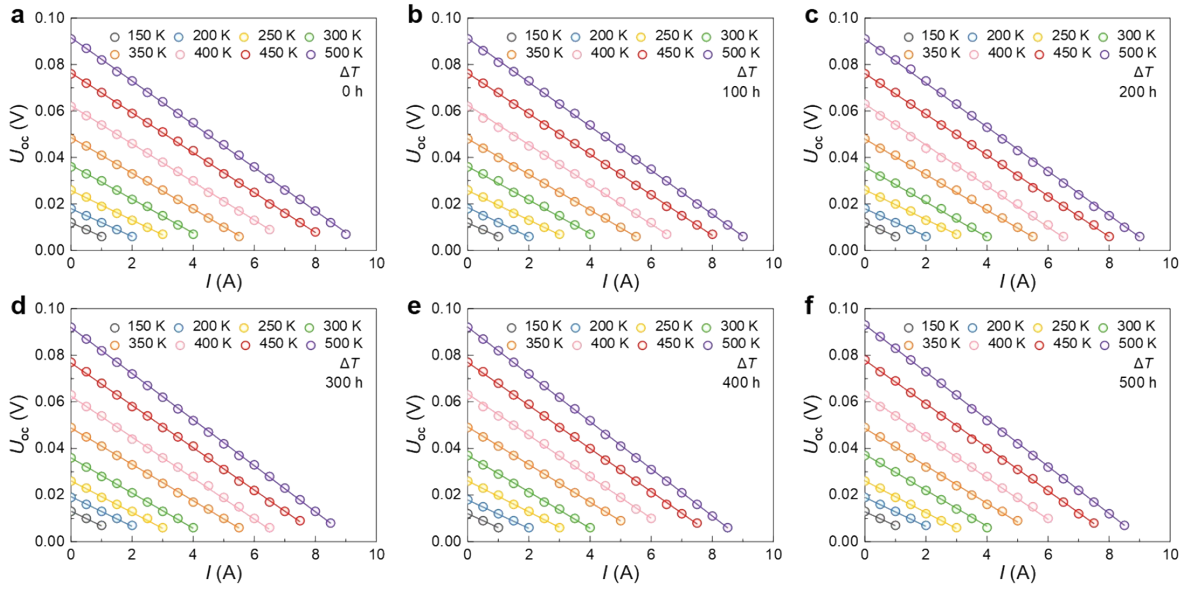
**Supplementary Figure S3.** The aging time dependence of the tensile strength for the Fe and FeCoNiCr junctions aged at 723 K.<sup>1</sup>



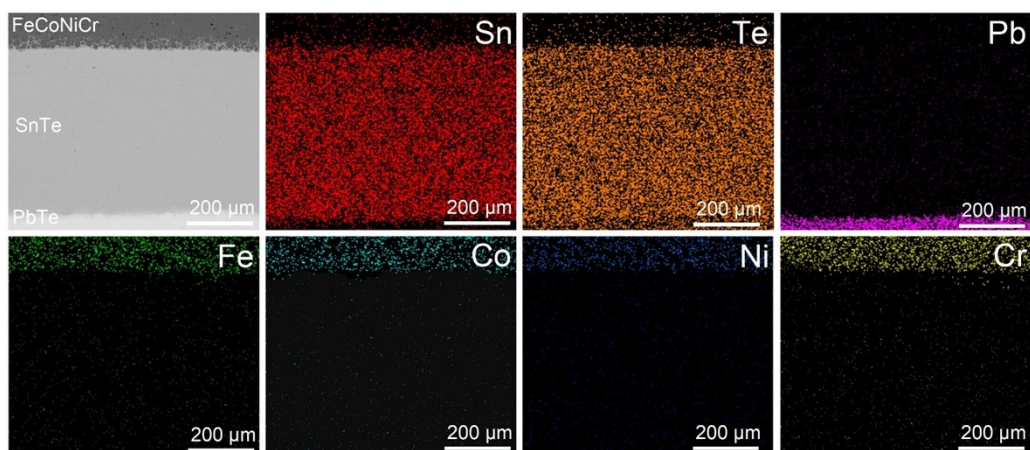
**Supplementary Figure S4.** The comparison between the measured  $U_{oc}$  and  $R_{in}$  and their simulated values under different  $\Delta T$ .



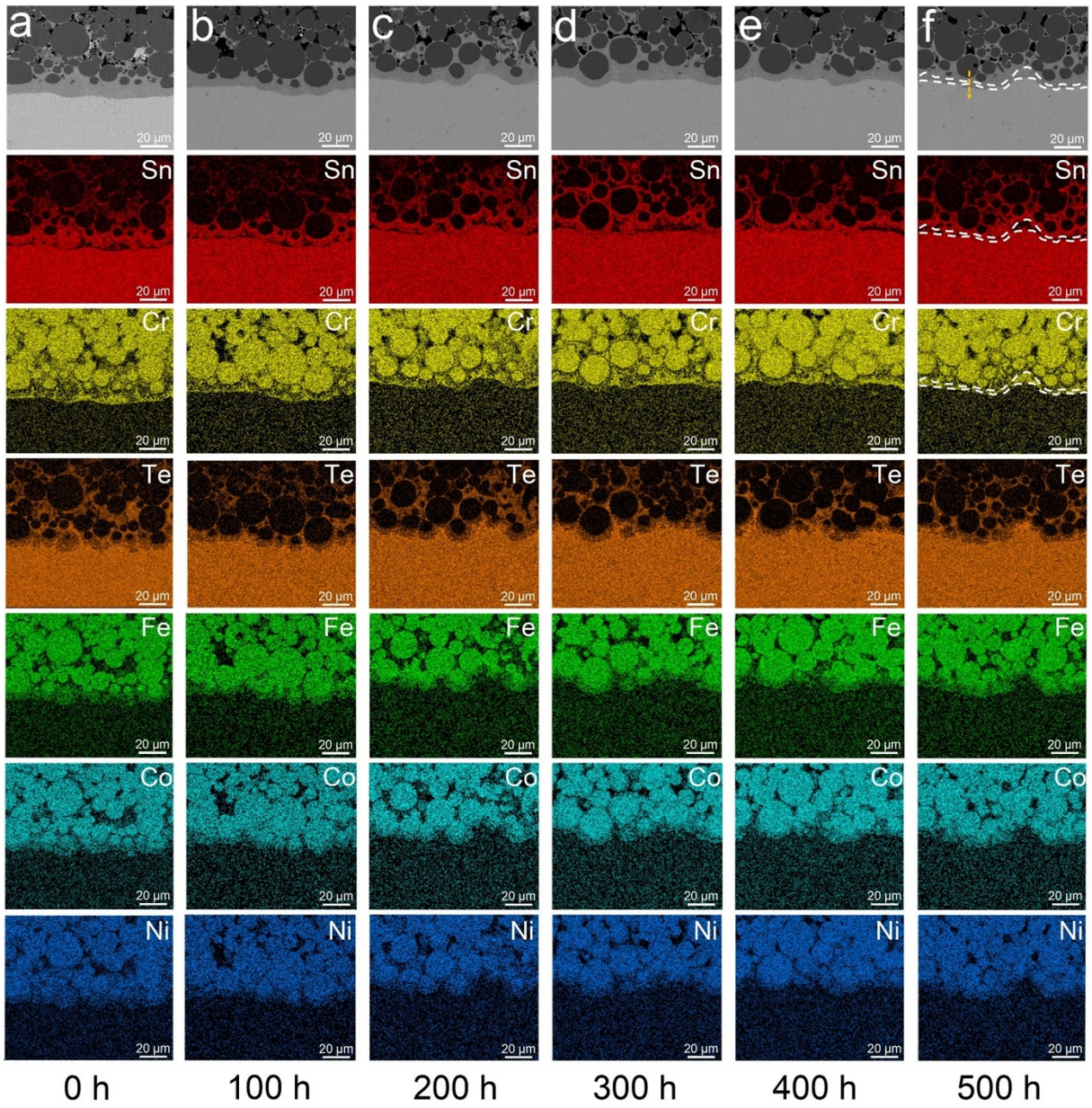
**Supplementary Figure S5.** Design of the simulation model for the TE leg.



**Supplementary Figure S6.** The  $U_{oc}$  of the TE leg at various  $\Delta T$  after different aging durations.



**Supplementary Figure S7.** SEM image and EDS elemental mappings of PbTe/SnTe/FeCoNiCr junction after sintering. The SnTe-PbTe interface exhibits both structural coherence and chemical stability. A pronounced particle size discrepancy between the FeCoNiCr and SnTe powders generated an interfacial transition region averaging  $170\pm 30$   $\mu\text{m}$  in width during powder compaction.



**Supplementary Figure S8.** SEM images and EDS elemental mappings of Fe, Co, Ni, Cr, Sn, and Te in PbTe/SnTe/FeCoNiCr junctions after aging at different durations.

Component	$zT$	Reference
$\text{Pb}_{0.93}\text{Na}_{0.04}\text{Sn}_{0.02}\text{Te}$	2.0	[2]
$\text{Pb}_{0.93}\text{Na}_{0.04}\text{Mn}_{0.02}\text{Te}$	2.1	[3]
$\text{Pb}_{0.95}\text{Na}_{0.04}\text{Te}_{0.97}\text{Se}_{0.03}$	2.2	[4]
$\text{Pb}_{0.94}\text{Na}_{0.03}\text{Eu}_{0.03}\text{Te}_{0.7}\text{Se}_{0.3}$	2.3	[5]
$\text{Pb}_{0.97}\text{Na}_{0.03}\text{Te}$	1.7	[6]
$\text{Pb}_{0.98}\text{Na}_{0.02}\text{Te}$	1.6	This work

**Supplementary Table S1.** A comparison of ZT values between the PbTe material used in this work and representative Na-doped PbTe systems reported previously.

Contact structure	$\rho_c$ ( $\mu\Omega$ cm <sup>2</sup> )	Reference
PbTe/ FeSb/Ag	1	[7]
PbTe/Fe <sub>0.8</sub> Sn <sub>0.2</sub>	3	[8]
PbTe/Co/Ag	5	[9]
PbTe/PbTe+Fe/Fe	7.6	[10]
PbTe/FeCo	10	[11]
PbTe/FeTe	11	[12]
PbTe/Fe	16	[12]
PbTe/Co-P	21.25	[13]
CoSb <sub>3</sub> /Nb	1	[14]
Mg <sub>3</sub> (Sb,Bi) <sub>2</sub> /Fe <sub>7</sub> Cr <sub>2</sub> Mg	2.5	[15]
MgAgSb/Co	2.5	[16]
Mg <sub>3</sub> (Sb,Bi) <sub>2</sub> /304SS	5.09	[17]
Mg <sub>3</sub> (Sb,Bi) <sub>2</sub> /Ti foil	5.5	[18]
TeSb/Ni <sub>0.5</sub> Te/Ni	9	[19]
Bi <sub>2</sub> Te <sub>3</sub> /Co-P	25	[20]
HH/Ag	38	[21]
Bi <sub>2</sub> Te <sub>3</sub> /Ni/Ag	40	[22]
PbTe/ SnTe/FeCoNiCr	3	This work

**Supplementary Table S2.** Interfacial resistivity for this work, with a comparison to the literature results.

Parameter	Value
Temperature of hot side	400~800 K
Temperature of cold side	300 K
Thickness of Cu electrode	0.3 mm
Electrical contact resistance of TE legs	6 $\mu\Omega$ cm <sup>2</sup>
Dimensions of TE leg	5×5×10 mm
Resistance of external load	10 <sup>^</sup> range(log <sub>10</sub> <sup>(0.0001)</sup> , 1/2, log <sub>10</sub> <sup>(0.1)</sup> ) $\Omega$
Thermal conductivity	400~245 W m <sup>-1</sup> K <sup>-1</sup> (300~800K)

**Supplementary Table S3.** Finite element simulation setting parameters.

Spectrum	Sn	Te	Cr	Fe	Co	Ni
(i)	0	0	24.99	24.65	25.52	24.84
(ii)	33.05	1.94	2.9	20.2	22.05	19.86
(iii)	1.48	53.75	44.77	0	0	0
(iv)	49.86	50.14	0	0	0	0

**Supplementary Table S4.** Point scanning result of the interface between FeCoNiCr barrier layer and SnTe after aging at 723 K for 500 h.

## Reference

1. S. Chen, Y. Wang, Y. Wang, W. Fan, J. Guo, J. Chen, Y. Jiang, R. A. A. Al-Yusufi and Z. A. Munir, *J. Alloys Compd.*, 2022, **905**, 164267.
2. F. Lv, Y. Zhong, X. Zhao, X. An, L. Lin, D. Ren, B. Liu and R. Ang, *Mater. Today Phys.*, 2023, **34**, 101061.
3. X. An, B. Tian, Q. Deng, H. Ma, W. Yuan, Z. He, R. Li, X. Tan, Q. Sun and R. Ang, *ACS Appl. Mater. Interfaces*, 2024, **16**, 4827–4835.
4. X. Zhao, B. Fu and R. Ang, *Adv. Funct. Mater.*, 2024, **34**, 2401582.
5. J. Zhou, Y. Wu, Z. Chen, P. Nan, B. Ge, W. Li and Y. Pei, *Small Struct.*, 2021, **2**, 2100016.
6. B. Cai, J. Li, H. Sun, L. Zhang, B. Xu, W. Hu, D. Yu, J. He, Z. Zhao, Z. Liu and Y. Tian, *Sci. China Mater.*, 2018, **61**, 1218–1224.
7. L. Yin, F. Yang, X. Bao, W. Xue, Z. Du, X. Wang, J. Cheng, H. Ji, J. Sui, X. Liu, Y. Wang, F. Cao, J. Mao, M. Li, Z. Ren and Q. Zhang, *Nat. Energy*, 2023, **8**, 665–674.
8. H. He, J. Song, R. Liang, G. Yan, Y. Geng, L. Hu, F. Liu, W. Ao and C. Zhang, *Small*, 2025, **21**, 2408864.
9. M. Liu, X. Zhang, J. Tang, Z. Chen, W. Li and Y. Pei, *Sci. Bull.*, 2023, **68**, 2536–2539.
10. A. Singh, S. Bhattacharya, C. Thinaharan, D. K. Aswal, S. K. Gupta, J. V. Yakhmi and K. Bhanumurthy, *J. Phys. D: Appl. Phys.*, 2009, **42**, 015502.
11. R. Chetty, P. Jood, M. Murata, K. Suekuni and M. Ohta, *Appl. Phys. Lett.*, 2022, **120**, 013501.
12. S. Chen, Y. Wang, Y. Wang, W. Fan, J. Guo, J. Chen, Y. Jiang, R. A. A. Al-Yusufi and Z. A. Munir, *J. Alloys Compd.*, 2022, **905**, 164267.
13. H.-C. Hsieh, C.-H. Wang, W.-C. Lin, S. Chakroborty, T.-H. Lee, H.-S. Chu and A. T. Wu, *J. Alloys Compd.*, 2017, **728**, 1023–1029.
14. J. Chu, J. Huang, R. Liu, J. Liao, X. Xia, Q. Zhang, C. Wang, M. Gu, S. Bai, X. Shi and L. Chen, *Nat. Commun.*, 2020, **11**, 2723.
15. X. Wu, Z. Han, Y. Zhu, B. Deng, K. Zhu, C. Liu, F. Jiang and W. Liu, *Acta Mater.*, 2022, **226**, 117616.
16. W. Zuo, H. Chen, Z. Yu, Y. Fu, X. Ai, Y. Cheng, M. Jiang, S. Wan, Z. Fu, R. Liu, G. Cheng, R. Xu, L. Wang, F. Xu, Q. Zhang, D. Makarov and W. Jiang, *Nat. Mater.*, 2025, **24**, 735–742.
17. L. Yin, C. Chen, F. Zhang, X. Li, F. Bai, Z. Zhang, X. Wang, J. Mao, F. Cao, X. Chen, J. Sui, X. Liu and Q. Zhang, *Acta Mater.*, 2020, **198**, 25–34.
18. Y. Fu, X. Ai, Z. Hu, S. Zhao, X. Lu, J. Huang, A. Huang, L. Wang, Q. Zhang and W. Jiang, *Nat. Commun.*, 2024, **15**, 9355.
19. X. Miao, W. Fan, S. Chen, Q. Zhang, D. An, Z. Wang, L. Hu, Z. A. Munir and C. Dun, *Chem. Eng. J.*, 2025, **505**, 159663.
20. C.-H. Wang, H.-C. Hsieh, Z.-W. Sun, V. K. Ranganayakulu, T.-W. Lan, Y.-Y. Chen, Y.-Y. Chang and A. T. Wu, *ACS Appl. Mater. Interfaces*, 2020, **12**, 27001–27009.
21. P. H. Ngan, N. Van Nong, L. T. Hung, B. Balke, L. Han, E. M. J. Hedegaard, S. Linderoth and N. Pryds, *J. Electron. Mater.*, 2016, **45**, 594–601.
22. A. K. Bohra, R. Bhatt, A. Singh, S. Bhattacharya, R. Basu, K. N. Meshram, S. K. Sarkar,

P. Bhatt, P. K. Patro, D. K. Aswal, K. P. Muthe and S. C. Gadkari, *Mater. Des.*, 2018, **159**, 127–137.